

Scientific article

Hyaluronic acid in the eggshell of *Salvator merianae* (Squamata: Teiidae)**Ácido hialurónico en la cáscara de huevo de *Salvator merianae* (Squamata: Teiidae)**

F.H. Campos-Casal*; E.I. Gomez; F.A. Cortez; S.N. Chamut

Cátedra Biología del Desarrollo, Facultad de Agronomía y Zootecnia, Universidad Nacional de Tucumán. Florentino Ameghino S/N. El Manantial, Tucumán, (T4104AUD), Argentina. *E-mail: fhccasal@gmail.com

Abstract

Eggshell is a multifunctional biological system in which minerals, fibril-forming biopolymers, and glycosaminoglycans coexist, whose combination produces materials with exceptional qualities and functional heterogeneity. In particular, glycosaminoglycans are characterized by their properties to produce viscoelastic hydrogels, control bacterial growth, and provide tissue resistance. In this work, we examined the eggshell surface of *Salvator merianae* with optical microscopy, transmission electron microscopy, and Raman vibrational spectroscopy. Histochemical examination using Alcian Blue combined with Periodic Acid-Schiff demonstrated a continuous glycosaminoglycan coating on the eggshell surface. Ultra-structurally this glycosidic coating exhibited an amorphous configuration with zones of different electron density. Besides, Raman spectroscopic analysis of this region showed representative vibrational bands of hyaluronic acid. A characteristic biopolymer coating for its high hydration capacity and rheological properties would be linked to the necessary hydric requirements for *S. merianae* embryonic development and would allow considering appropriate parameters for the artificial incubation of eggs in this species. Determining the biomolecules that make up the eggshell of reptiles could provide new biological material for research in the emerging field of biomaterials.

Keywords: Biomaterials; Glycosaminoglycans; Raman spectroscopy; Reptiles.

Resumen

La cáscara de huevo es un sistema biológico multifuncional en el que coexisten minerales, biopolímeros formadores de fibrillas y glicosaminoglicanos, cuya combinación produce materiales con cualidades excepcionales y heterogeneidad funcional. En particular, los glicosaminoglicanos son característicos por sus propiedades para producir hidrogeles viscoelásticos, controlar el crecimiento bacteriano y proporcionar resistencia tisular. En este trabajo examinamos la superficie de la cáscara de huevo de *Salvator merianae* con microscopía óptica, microscopía electrónica de transmisión, y espectroscopía vibracional Raman. El examen histoquímico utilizando Azul Alcian combinado con Ácido Peryódico de Schiff demostró una cubierta ininterrumpida de glicosaminoglicanos en la superficie de la cáscara. Ultraestructuralmente este revestimiento glicosídico exhibió una configuración amorfa con zonas de diferentes electrodensidades. En adición, el análisis espectroscópico Raman de esta región evidenció bandas vibracionales representativas del ácido hialurónico. Una cobertura de biopolímeros característicos por su elevada capacidad de hidratación y propiedades reológicas, estaría vinculada con los requerimientos hídricos necesarios para el desarrollo embrionario de *S. merianae* y permitiría considerar parámetros apropiados para la incubación artificial de los huevos en esta especie. Determinar las biomoléculas que conforman la cáscara de huevo de los reptiles podría proporcionar un nuevo material biológico para investigar en el campo emergente de los biomateriales.

Palabras clave: Biomateriales; Glicosaminoglicanos; Espectroscopía Raman; Reptiles.

Introduction

Through millions of years of evolution, reptiles have developed a peculiar heterogeneity of reproductive patterns and, consequently, strategies necessary to adapt to the land habitat (Reisz, 1997). The amniote egg represents an outstanding innovation that has linked the composition and conformation of the shell with metabolism, development,

and embryonic survival (Hallmann and Griebeler, 2015). This adaptation against desiccation implies that the egg must contain all the necessary components to guarantee extrauterine development (Schmidt-Nielsen, 1997). To ensure this dynamic challenge, the shell controls the exchange of water and gases, protects the embryo from microbial attack, and is a source of minerals (Osborne and Thompson, 2005; Chang and Chen, 2016).

Received: 09/26/2020; Accepted: 11/24/2020.

The authors declare to have no conflict of interests.

Considering the structural organization of the eggshell and the sensitivity to the hydric environment of the nest, it is possible to distinguish eggs with strongly calcified eggshells, characteristic of some gekkotan species (Schleich and Kästle, 1988; Pike *et al.*, 2012) and eggs with flexible shell or parchment-shelled eggs, distinctive of lizards and snakes (Packard *et al.*, 1982b; Hirsch, 1983).

Recently it was demonstrated that the eggshell of *Salvator merianae* has an organic and inorganic composition notably different from that described for the parchment-shelled eggs of reptiles (Campos-Casal *et al.*, 2020). It was found the presence of hydroxyapatite in the deep section of the shell, compact and alveolar fibers, and although it was not characterized at the molecular level, the histological analysis revealed a glycoprotein coating on the outer surface of the egg (Campos-Casal *et al.*, 2020).

Eggshells are a perfect example of the organic-inorganic concept made up of multifunctional biopolymers and biominerals, recognized for their lightweight, strong, and resistant structure (Fratzl and Weinkamer, 2007). The remarkable toughness and damage tolerance of these biological materials are conferred through the hierarchical assembly of their architectures, and multiscale components (Weinkamer and Fratzl, 2011). The organic components that makeup biopolymers are protein-forming polypeptides (collagen, keratin, elastin, resilin, fibroin, abductin), and glycosaminoglycans [GAGs; (Chen *et al.*, 2012; Scott and Panitch, 2013)].

GAGs are a small family of polymers consisting of unbranched chains of repeated disaccharide units containing hexosamine, and hexuronic acid or hexose (Ellis *et al.*, 2009). Because of their tendency to occupy large domains in aqueous solution, GAGs are responsible for the structural and mechanical functions of the extracellular matrix [ECM; (Raman *et al.*, 2005)].

There are two major types of GAGs. Sulfated GAGs include chondroitin sulfate, dermatan sulfate, keratan sulfate, heparin, and heparan sulfate; while hyaluronic acid (HA) or hyaluronan is the only non-sulfated GAG (Gandhi and Mancera, 2008). HA is a biopolymer composed of a disaccharide sequence of *N*-acetylglucosamine (GlcNAc) and *D*-glucuronic acid (GlcA) linked by alternating glycosidic bonds β -1 \rightarrow 4, and β -1 \rightarrow 3 (Nusgens, 2010). Due to the high number of car-

boxyl and hydroxyl groups, HA is a highly hydrophilic biomaterial, that forms a gel-like structure in aqueous solution as a result of intermolecular interaction among linear polymers (Zhu *et al.*, 2017). In terms of water transport, diffusion, and ion exchange, the physiological functions of tissues are determined by the concentration of HA and its molecular weight (Dicker *et al.*, 2014). Besides, this polymer has shown to possess significant bacteriostatic properties (Romanò *et al.*, 2017; Chen *et al.*, 2019). The remarkable viscoelastic and water retention properties of HA, in addition to its biocompatibility, biodegradability, and null immunogenicity, have amplified the attractiveness of this biomolecule in the field of tissue engineering (Fallacara *et al.*, 2018).

The study of bird eggshells has been a focus of interest in the emerging field of biomaterials (Baláž, 2014; Sah *et al.*, 2016) for its content of GAGs (Liu *et al.*, 2014), collagen fibers (Zhao and Chi, 2009), and keratins (Nys *et al.*, 2001). Particularly high proportions of HA have been shown in the calcified fraction in the eggs of this animal group (Heaney and Robinson, 1976; Liu *et al.*, 2014).

Although reptile eggshells have been extensively studied, the focus has been on the general morphology of their structure, and on the mechanisms of mineralization (Kusuda *et al.*, 2013; Hallmann and Griebeler, 2015). However, at present, there is insufficient information available in terms of structural characterization at the multi-scale level, compositional analysis, and mechanical properties associated with the biomaterials that make up the eggshell of reptiles (Chang and Chen, 2016).

In this context, investigating and identifying the constituent biopolymers of *S. merianae* eggshells would offer alternative designs for the multiscale study of new multifunctional biological materials. The structural particularities, chemical composition (Campos-Casal *et al.*, 2020), and high hydric requirements of the *S. merianae* egg (Manes, 2016), establish criteria for investigating the molecular nature of the glycoprotein coating of the eggshell. In perspective, knowing the conformation of this physiological structure, and the behavior of its structural components would allow establishing application parameters for the development of artificial incubation technologies.

In the present work, we analyze the ultrastructure of the surface of the recently oviposited egg from *S. merianae* with transmission electron mi-

croscopy (TEM), we examine the superficial glycosidic component with optical microscopy and we determine the molecular fingerprint of the glycoprotein covering using Raman spectroscopy.

Materials and methods

Biological material

To exclude possible modifications in the structure and chemical composition of the shells associated with incubation or embryonic development, eggs recently oviposited in a perfect preservation status of conservation were used. The eggs ($n = 24$) were taken from six nests built by *S. merianae* females (with at least two previous egg-layings). The average weight of the females was 4 kg, and the average snout-vent length > 35 . The animals were housed in the experimental lizard farm of the Facultad de Agronomía y Zootecnia of the Universidad Nacional de Tucumán, located at Finca El Manantial ($26^{\circ} 51' S$, $65^{\circ} 17' W$), province of Tucumán, Argentina. The protocols for the handling and care of the animals were carried out by the "Guide for the care and use of laboratory animals" (Committee for the update of the guide for the care and use of laboratory animals, 2011). All experiments performed were approved by the ethics committee of the Research Council of the Universidad Nacional de Tucumán (CIUNT).

Optical microscopy

For the histochemical studies, 12 whole eggs were fixed in 4% formaldehyde solution in phosphate-buffered saline at pH 6.8 (Suvarna *et al.*, 2008) for 24 h at $4^{\circ} C$. Small pieces of shells from each egg ($n = 24$) were dehydrated in ethyl alcohol, diaphanized in xylene, included in paraffin-celloidin and serially sectioned at $8 \mu m$.

For the determination of the GAGs, the sections were stained for 15 minutes in a solution of 1% Alcian Blue 8GX (AB; Sigma-Aldrich, Buenos Aires, Argentina) pH 2.5 (Suvarna *et al.*, 2008). After washing in distilled water, the shell samples were stained with a Periodic Acid-Schiff (PAS) kit (Biopur, Rosario, Argentina). The sections were then dehydrated in absolute ethyl alcohol and mounted in acrylic resin (Biopack, Buenos Aires, Argentina).

The samples were photographed with an Olympus BH2 Microscope (Olympus Corporation, Tokyo, Japan) equipped with a Canon Eos Rebel

T3i digital camera (Canon Corporation, Tokyo, Japan).

Electronic microscopy

Small pieces of eggshells ($n = 12$) were fixed in half-concentration Karnovsky's fixative [2.5% glutaraldehyde, 2% formaldehyde, pH 7.4; (Karnovsky, 1965)] for 24 h at $4-5^{\circ} C$, post-fixed with 2% osmium tetroxide (Ted Pella, California, U.S.A), dehydrated in increasing concentrations of acetone and included in Spurr resin (Ted Pella, California, U.S.A). The ultrasections were contrasted with 2% Uranyl Acetate (Ted Pella, California, U.S.A) and observed with Zeiss Libra 120 Transmission Electron Microscope (Carl Zeiss, Oberkochen, Germany) controlled with Win TEM user interface and system software (Carl Zeiss).

Raman spectroscopy and statistics

The spectroscopic examination was performed with a confocal Raman Microscope DXR (Thermo Fisher Scientific, Waltham, Massachusetts, USA) equipped with an excitation wavelength of 780 nm at 24 mW of power (5^{-1} spectral resolution). A confocal aperture of $50 \mu m$ was used for data collection. The samples were focused with a 20x objective. All measurements were made at room temperature.

The outer surface of the recently oviposited egg of *S. merianae* exhibits irregular plaques separated by fissures (Campos-Casal *et al.*, 2020). This configuration was considered to establish the five consecutive sampling points on the shell surface ($n = 6$). Indeed, from left to right (3C), points one, two, four, and five correspond to the samples taken in two consecutive plaques. Point three was sampled in the center of a fissure (3C). Each sampling point produced an individual spectrum, which was acquired by accumulating 100 exposures with an exposure time of 5 s each.

A total of 30 spectra were measured from the samples. The spectral profile of most of the sampled points proved to be very similar to each other, allowing the generation of a single average-spectrum representative of the overall spectral behavior of the plaques and fissures. The spectral adding and baseline correction of the average-spectrum were performed with the optical spectroscopy software Spectragryph. The overlapping frequencies were mathematically decomposed with the Origin Pro software, using the Voigt function.

The statistical analysis was performed with

In foStat software (Di Rienzo *et al.*, 2018). The *t*-test was used to compare the HA distribution on the plaques and the fissures using the vibrational frequencies and the Raman intensities of the average-spectrum.

Results and discussion

Optical microscopy and surface ultrastructure

Microscopic examination of the AB pH 2.5 and PAS stained sections exhibited an intense GAGs coating on the outer surface of the *S. merianae* eggshell (1).

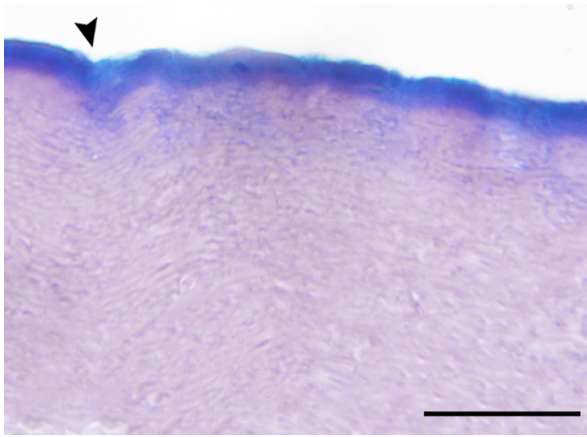


Figure 1. Light micrograph of a cross-section through eggshell stained with AB pH 2.5 and PAS showing a continuous coating of glycoproteins on the outer surface. The arrowhead points to a fissure. Scale bar 30 μm .

Ultrastructural analysis showed two different regions, recognizable by their amorphous appearance and fibrillar content (Figures 2A and 2B). Thus, the outermost section forms a continuous cover composed of different electrodense zones (Figures 2A and 2B). In particular, under the free surface of the shell, a band with moderate electronic density was observed (Figure 2B). Below this outer cover, small alveolar fibers (Figure 2A) were observed included in a matrix with a granular configuration (Campos-Casal *et al.*, 2020). However, crystalline structures were not recognized, a characteristic incompatible with the idea that supports the presence of calcium carbonate in soft and hard shells of reptiles (Packard and DeMarco, 1991; Choi *et al.*, 2018). It has been shown that the only biomineral present in the eggshell of *S. merianae* is hydroxyapatite, located in the deep section of the eggshell (Campos-Casal *et al.*, 2020).

Raman spectroscopy

Raman spectroscopy has proven to be an outstanding tool for the structural characterization of glycosaminoglycans (Arboleda and Loppnow, 2000). Raman frequencies assignments for HA and its monomeric components have generally been reported using purified biomolecules (Reineck *et al.*, 2003; Meziane-Tani *et al.*, 2006; Synytsya *et al.*, 2011). However, in complex biological systems, the Raman spectrum of numerous biopolymers may exhibit shifts in the position of

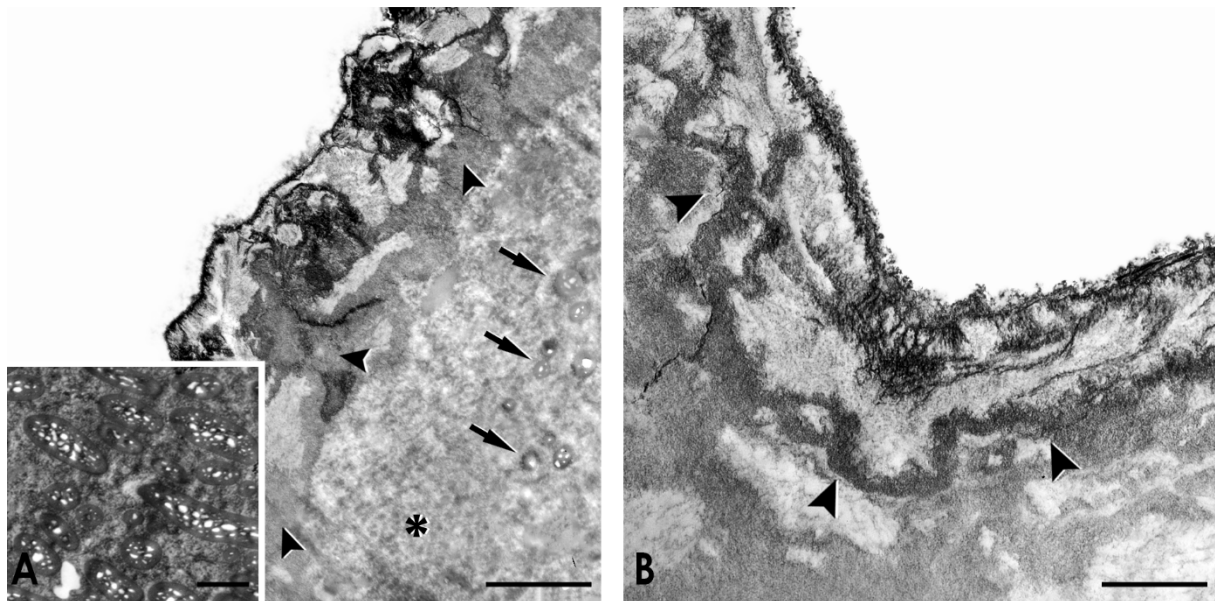


Figure 2. TEM photographs of the eggshell surface of *S. merianae*. A) Note the electrodense zones (arrowheads) and the granular matrix (asterisk) with small alveolar fibers cross-sectioned (arrows). The insert shows superficial alveolar fibers surrounded by interfibrillar material. Scale bar 2 μm . B) Detail of the moderate electron density band (arrowheads) underlying the surface of the shell. Scale Bar 1 μm . In both images, the outside of the eggshell is on top.

their frequencies ($\pm 1\text{-}5^{-1}$) as a result of structural and conformational alterations (Bergholt *et al.*, 2016).

The analysis of the average Raman spectra of plaques and fissures of the eggshell of *S. merianae* are shown in Figures 3A and 3B. The main characteristic bands of the HA were determined in two spectral windows: 600-1,800 cm^{-1} (Figure 3A), and 2,800-3,000 cm^{-1} (Figure 3B). The Amide I (AmI) and Amide III (AmIII) domains of the HA can be easily distinguished along with bands associated with carbohydrate chains and several amino acid vibrations.

The spectral section between 610-683 cm^{-1} contains bands assigned to the out-of-plane vibration modes of the groups CCO, CCH, C=O, and CO. Although these vibrations have been assigned to HA (Synytsya *et al.*, 2011), the Raman spectral analysis of the GlcA suggested that the bands at 629 cm^{-1} and 665 cm^{-1} would be distinctive of this constituent monomer of HA (Meziane-Tani *et al.*, 2006).

The deconvolution of the spectral range between 850-980 cm^{-1} (Figures 4A and 4B) evidenced in the average-spectrum of the plaques and the fissures the overlapping of frequencies at 864 cm^{-1} , 899 cm^{-1} , 923 cm^{-1} , 951 cm^{-1} , 960 cm^{-1} , and 970 cm^{-1} , vibrations typical of the bonds of the anomeric skeletal configuration (α or β), and the glycosidic bonds (Yuen *et al.*, 2009). These frequencies are similar to those reported for HA (Bansil *et al.*, 1978; Barret and Peticolas, 1979).

In general, the main spectral features of carbohydrate chains are associated with C-O stretching coupled with C-O-H deformation modes, which can be observed as a triplet of peaks at 1,025-1,045 cm^{-1} ; 1,080-1,100 cm^{-1} and 1,110-1,152 cm^{-1} respectively [Figure 3A; (Bansil *et al.*, 1978; Katsumata *et al.*, 1996)]. In particular, the region covering the range of 1,000 cm^{-1} and 1,100 cm^{-1} was associated with the vibrations of the saccharide molecular bonds that correlate with the C-O-C, C-C-C, and C-C-O stretching of the pyranose ring of the GAGs (Parker, 1983). Our spectra exhibited bands of C-C and

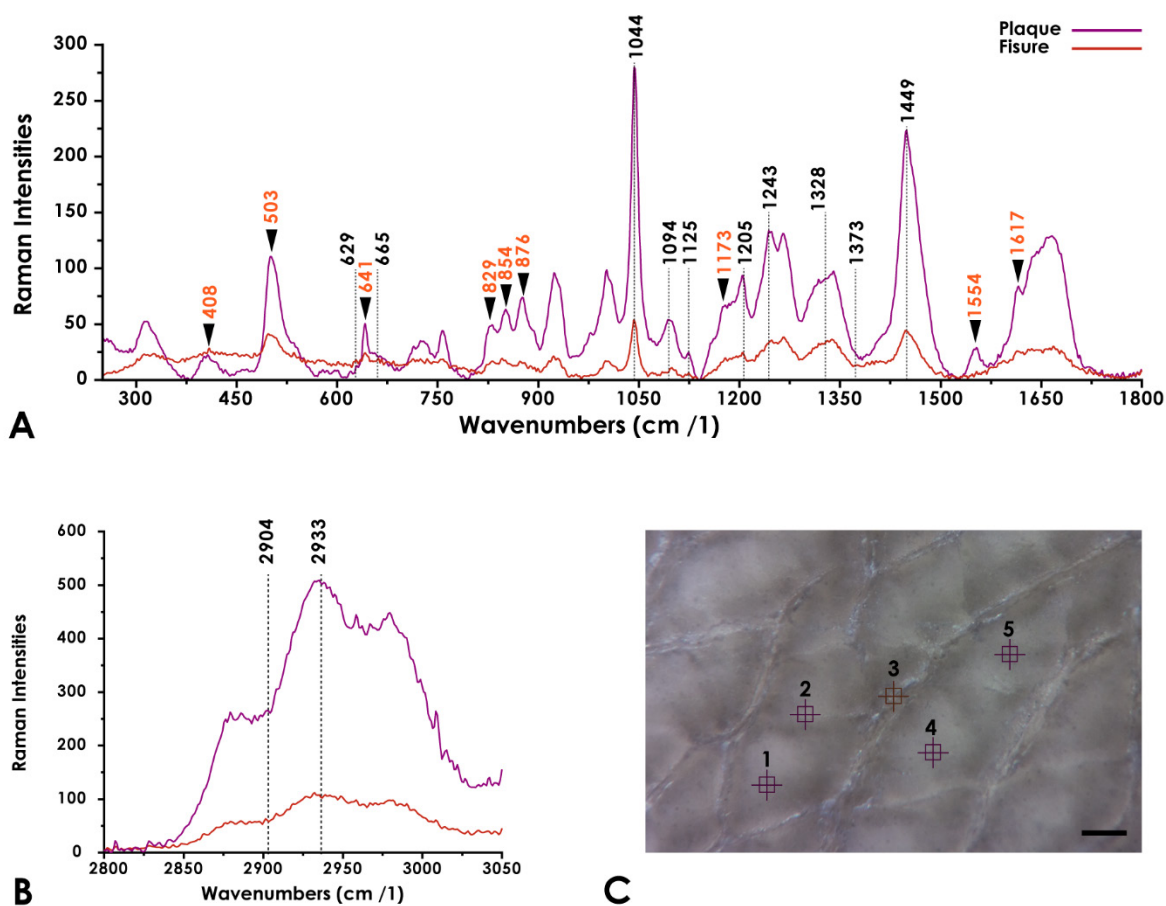


Figure 3. Average-spectrum of plaques and fissures. A) Representative Raman average-spectra between 300-1,800 cm^{-1} . The graph indicates the tentative assignments of the HA in plaques and fissures. Amino acid frequencies are indicated with an arrowhead. B) Representative Raman average-spectra between 2,800-3,000 cm^{-1} . C) Microphotography of the outer surface of the eggshell indicating the five sampling points corresponding to average-spectra in images A and B. Scale Bar 100 μm .

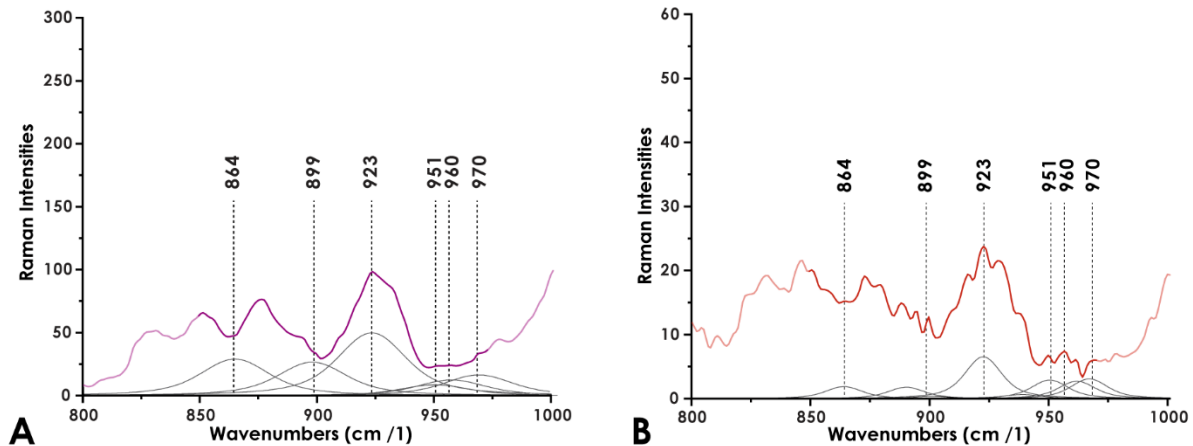


Figure 4. Decomposition of the Raman spectra between 850-980 cm^{-1} of plaques (A) and fissures (B).

C-O stretching vibrations at $1,044 \text{ cm}^{-1}$, bending vibration of C-OH from the acetyl group ($\sim 1,094 \text{ cm}^{-1}$) and a peak formed by bending vibrations of C-OH and C-H ($1,125 \text{ cm}^{-1}$). In particular, the frequency $\sim 1,094 \text{ cm}^{-1}$ has been assigned to the symmetric and antisymmetric vibrations of the β -glycosidic bonds (Sekkal *et al.*, 1995; Alkrad *et al.*, 2003) of the HA. Besides, the $\sim 1,125 \text{ cm}^{-1}$ band is considered an outstanding marker for the determination of this biopolymer, considering that this vibration is exclusive of glucose derivatives (Bansil *et al.*, 1978). A medium intensity peak, representative of bending vibrations of CH_2 at $1,205 \text{ cm}^{-1}$, was also determined in both average spectra.

On the other hand, it was possible to establish a second spectral region (Fig. 3A) corresponding to the AmIII complex ($1,215$ - $1,350 \text{ cm}^{-1}$). In effect, in this vibrational segment, bands were determined at $1,243 \text{ cm}^{-1}$ belonging to the irregular or disordered domains (random coils), and at $1,328 \text{ cm}^{-1}$ features of the saccharide moiety reported for the *N*-acetyl-monosaccharides (Bansil *et al.*, 1978; Oleinikov *et al.*, 1999). On the other hand, the vibrations representative of the asymmetric and symmetric bending of the C-H₃ groups of the HA were distinguished at $1,373 \text{ cm}^{-1}$ and $1,449 \text{ cm}^{-1}$ respectively (Kotzianova *et al.*, 2015).

The broad AmI spectral region between $1,600 \text{ cm}^{-1}$ and $1,700 \text{ cm}^{-1}$ (Kitagawa and Hirota, 2006; Rygula *et al.*, 2013), observed in our spectra, consists of overlapping vibrations related to carbonyl group stretching reported for HA (Kotzianova *et al.*, 2015). The spectral deconvolution of this region (Figs. 5A and B) in both average-spectra of the eggshell revealed vibrations at $1,600 \text{ cm}^{-1}$, $1,630 \text{ cm}^{-1}$, $1,636 \text{ cm}^{-1}$, $1,655 \text{ cm}^{-1}$ and $1,664 \text{ cm}^{-1}$ respectively. In particular, the frequencies of the shoulders at $\sim 1,600 \text{ cm}^{-1}$ and $\sim 1,630 \text{ cm}^{-1}$, have

been suggested as representative of the asymmetric COO^- stretching of the HA (Synystsyia *et al.*, 2011; Essendoubi *et al.*, 2016). Also, the band at $1,655 \text{ cm}^{-1}$ would distinguish the vibrations of the C=C groups and the C=O groups of AmI of this biopolymer (Synystsyia *et al.*, 2011).

The second spectral window analyzed between $2,800$ - $3,000 \text{ cm}^{-1}$ (Figure 3B), contains two bands at $2,904 \text{ cm}^{-1}$ and $2,933 \text{ cm}^{-1}$ respectively. Indeed, these vibrations represent the C-H and N-H stretches of the HA (Donghui *et al.*, 2006; Essendoubi *et al.*, 2016).

In addition to the characterization of the amides bands of HA, there are additional characteristics in the Raman spectra that allow the description of the protein environment as a function of the amino acid side chains (Rygula *et al.*, 2013).

Indeed, Figure 3A shows a prominent Raman band $\sim 503 \text{ cm}^{-1}$, which can be assigned to the S-S stretching mode of cysteine (Cys) and cystine residues (Widjaja and Garland, 2010). This vibration confirms that the conformation of the C-C-S-S-C group is gauche-gauche-gauche, largely stable conformation (Edwards *et al.*, 1998). Two other pure components vibrations associated with the C-S stretching of Cys and cystine residues are resolved with a prominent band at 641 cm^{-1} and a shoulder at $\sim 663 \text{ cm}^{-1}$ respectively (Akhtar and Edwards, 1977; Widjaja and Garland, 2010). In our spectra, an overlap of the $\sim 663 \text{ cm}^{-1}$ band with the frequency at 665 cm^{-1} of the HA could be observed.

On the other hand, the characteristic Fermi doublet of the tyrosine (Tyr) is distinguished at $829/854 \text{ cm}^{-1}$, along with two additional vibrations at $1,173 \text{ cm}^{-1}$ and $1,617 \text{ cm}^{-1}$ (Zhu *et al.*, 2011). Finally, the characteristic vibrations of proline (Pro) and hydroxyproline (Hyp) were recognized at 408

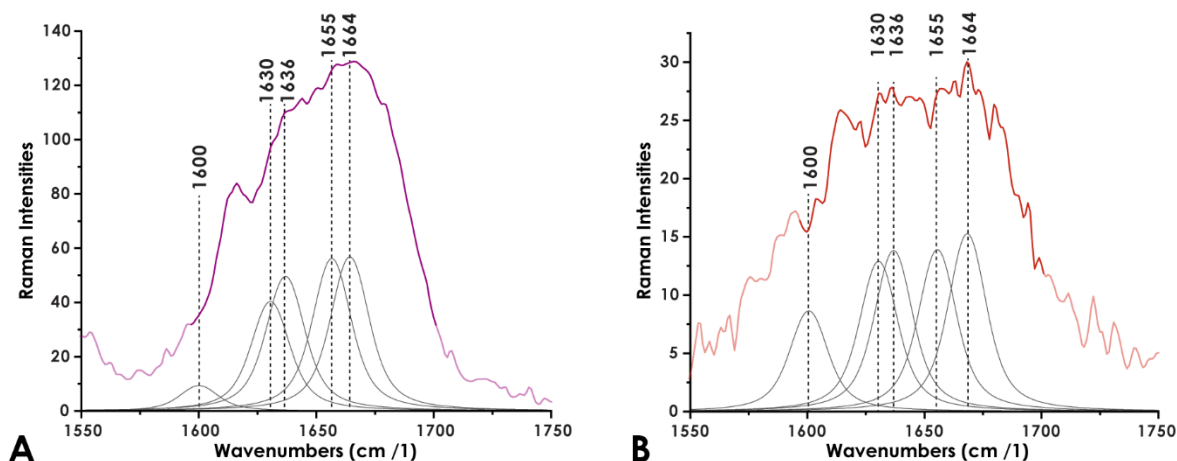


Figure 5. Decomposition of the Raman spectra of plaques (A) and fissures (B) corresponding to the vibration of the AmI complex.

cm^{-1} , 876 cm^{-1} , and $1,554 \text{ cm}^{-1}$ respectively (Zhu *et al.*, 2011).

The comparison of the relative intensities of the HA bands in the average-spectrum of the plaques and the fissures using the *t*-test indicates the absence of significant differences ($P = 0.4308$) in the distribution of HA and provides additional evidence to the histochemical studies, confirming that this biopolymer forms a continuous biofilm on the outer surface of the eggshell of *S. merianae*.

Many of the physiological effects of HA are related to its molecular weight (Hascall *et al.*, 2004; Medina *et al.*, 2006). Indeed, the HA of low molecular weight stimulates gene expression in macrophages, chondrocytes and some epithelial cells (Euppayo *et al.*, 2015; Jariyal *et al.*, 2020). On the contrary, the HA of high molecular weight characteristic for its viscoelastic properties (Gřundělová *et al.*, 2015) modulates the hydration of tissues, the osmotic balance (Salwowska *et al.*, 2016) and organizes the ECM (Manou *et al.*, 2019).

Raman spectroscopic studies of the HA with different molecular weights showed that the intense peak observed at $\sim 1,661 \text{ cm}^{-1}$ in the HA of 1,200 kDa reveals a remarkable widening and reduction in the spectral intensity compared to the HA of 31 kDa (Alkrad *et al.*, 2003). By analogy, the band at $1,664 \text{ cm}^{-1}$ in the average-spectrum of the plaques and the fissures, would be similar to the vibrational profile of the HA of high molecular weight described in those studies. Although the results presented here do not offer information related to the molecular weight of HA on the outer surface of the eggshell of *S. merianae*, it is remarkable that the vibrational frequency in our spectra at $1,243 \text{ cm}^{-1}$ and $1,664 \text{ cm}^{-1}$ are characteristic of the irregular or disordered domains of the AmIII and AmI com-

plex respectively (Rizo *et al.*, 2016). Although being a linear molecule, in aqueous solution, the HA of medium and high molecular weight show an expanded random coil conformation (Chakrabarti and Park, 1980; Scott *et al.*, 1991) optimal formation that provides local rigidity and high viscosity (Ingr *et al.*, 2017). Also, the size of the random coils can be modified by the pH and the concentration of salts in the medium, characteristics of a flexible polyelectrolyte (Lapçik *et al.*, 1998), capable of bridging transient hydrogens with water molecules (Almond, 2005; Blundell *et al.*, 2006). *In vivo* studies using Raman spectrography have shown that high molecular weight HA applied to skin samples remains on the surface forming a film that prevents water loss by evaporation (Essendoubi *et al.*, 2016).

Several polymers studied as antibacterial coatings, HA shows a proven ability to produce biofilms capable of reducing bacterial adhesion (Romanò *et al.*, 2017). Research related to the bacteriostatic effect of HA showed that this biopolymer with high molecular weight presents significant antiadhesive and inhibiting properties of bacterial growth (Pirnazar *et al.*, 1999; Chen *et al.*, 2019). Similar results were obtained by Carlson *et al.* (2004) comparing the bacteriostatic properties of HA with collagen Type I and hydroxyapatite, materials widely used in the manufacture of biomatrixes.

Considering the high sensitivity of the *S. merianae* egg to variations in the hydric environment of the nest and the absence of a calcareous coating (Campos-Casal *et al.*, 2020), the HA cover in a hydrated environment would create a viscoelastic hydrogel that also to preserve the developing embryo against desiccation, it would participate

in the protection, lubrication, and stabilization of the shell surface. Besides, due to its high molecular weight and its rheological properties, HA would form a stable biofilm, with characteristics of a semi-plastic fluid (Sudha and Rose, 2014), adaptable to the volumetric changes experimented by eggs with a flexible shell during incubation (Andrews, 1997). As we have indicated, studies related to the chemical composition of the *S. merianae* egg revealed a band of hydroxyapatite located in the deep zone of the shell (Campos-Casal *et al.*, 2020). Thus, considering the physicochemical characteristics of the incubation environment (Manes, 2016), it would be fair to consider that HA and hydroxyapatite could work synergistically to protect the egg against bacterial invasion. The presence of HA as a bioconstituent in reptile eggshell has not been previously reported. However, in birds, this biopolymer is abundant in the shell membranes, and the calcified matrix (Liu *et al.*, 2014; Vuong *et al.*, 2017).

Sexton *et al.* (2005) compared the amino acid distribution of eggshells from 24 lizard species, 6 snake species, and 4 external groups, including birds eggshells, and determined that eggs with flexible shells, such as *S. merianae*, contain significantly higher levels of Pro and Tyr compared to rigid shells. As we have shown, the vibrational frequencies of both amino acids are present in the eggshell of *S. merianae*. Significantly, collagen contains high proportions of Hyp, Pro and glycine (Soroushanova *et al.*, 2019), a biopolymer which in interaction with GAGs gives the distinctive mechanical resilience of the ECM (Holmes *et al.*, 2018).

Studies of the structure and mechanical properties of the Taiwan cobra snake eggshells (*Naja atra*) showed that the flexible eggshells of this reptile behave like a highly extensible elastomer; quality determined by the presence of keratin and collagen fibers (Chang and Chen, 2016). Likewise, collagen I, V, and X have been characterized in the eggshell of birds (Arias *et al.*, 1991).

Scanning electron microscopy analysis showed that the *S. merianae* eggshell is made up mostly of alveolar fibers, and a double layer of compact fibers, both immersed in an amorphous interfibrillar matrix (Campos-Casal *et al.*, 2020). On the other hand, the elemental composition of the *S. merianae* eggshell using energy-dispersive X-ray spectroscopy determined a high sulfur content in the surface layer (Campos-Casal *et al.*, 2020), higher

than that reported for eggs of other reptiles with calcified shells (Choi *et al.*, 2018). Although the ultrastructural studies only provide morphological evidence, it is reasonable to consider that the Pro and Hyp amino acid residues determined in the Raman spectra in the present work are representative of collagen fibers. In complex biological systems such as ECM, HA provides mechanical stability to collagen fibers (Wang *et al.*, 2010). On the other hand, considering that sulfur is usually bound to proteins associated with keratin (Rogers *et al.*, 2006), sulfur amino acids such as Cys and its dimer characterized in our spectra, offer consistent evidence to consider keratin and/or sulfated GAGs as constitutive biopolymers of the *S. merianae* eggshell.

A hydrophilic HA covering and protective viscoelastic on the outer surface of the *S. merianae* eggshell exposes a new perspective to establish correlations between the conditions of humidity and incubation temperature. Indeed, both physical parameters are substantial to develop artificial incubation technologies with a productive impact. On the other hand, the results presented here provide complementary evidence on the adaptations by which reptile eggs and embryos control the exchange of water with the incubation environment.

Conclusions

For the first time, an HA coating is identified in the eggshell of a reptile. The qualities of HA to maintain conformational rigidity and hydrophilicity; added to the ability to absorb impacts and interact with other GAGs and fibers of the ECM make it an important biomaterial. Therefore, the eggshell of *S. merianae* could offer an innovative platform for the study of structural, extensible, and lightweight biomaterials.

Acknowledgements

This paper has been partially funded by PIUNT Project 26/A605 to the Secretaría de Ciencia, Arte e Innovación Tecnológica of the Universidad Nacional de Tucumán. We are especially grateful to Dra. María Rosa Álvarez and Licenciada Doly Chemes of Laboratorio de Espectroscopía Raman, (LERA-CONICET) for their technical assistance during Raman measurements. We also thank to Dr. Mario Fortuna and Mg. Osvaldo Arce for their suggestions.

References

- Akhtar W., Edwards H.G. (1997). Fourier-transform Raman spectroscopy of mammalian and avian keratotic biopolymers. *Spectrochimica Acta. Part A, Molecular and Biomolecular Spectroscopy* 53 (1): 81-90.
- Alkrad J.A., Mrestani Y., Stroehl D., Wartewig S., Neuberger R. (2003). Characterization of enzymatically digested hyaluronic acid using NMR, Raman, IR, and UV-Vis spectroscopies. *Journal of Pharmaceutical and Biomedical Analysis* 31 (3): 545-550.
- Almond A. (2005). Towards understanding the interaction between oligosaccharides and water molecules. *Carbohydrate Research* 340 (5): 907-20.
- Andrews R.M. (1997). Evolution of viviparity: variation between two sceloporine lizards in the ability to extend egg retention. *Journal of Zoology* 250: 579-595.
- Arboleda P.H., Loppnow G.R. (2000). Raman spectroscopy as a discovery tool in carbohydrate chemistry. *Analytical Chemistry* 72 (9): 2093-2098.
- Arias J.L., Fernandez M.S., Dennis J.E., Caplan A.I. (1991). Collagens of the chicken eggshell membranes. *Connective Tissue Research* 26 (1-2): 37-45.
- Baláz M. (2014). Eggshell membrane biomaterial as a platform for applications in materials science. *Acta Biomaterialia* 10 (9): 3827-3843.
- Bansil R., Yannas I.V., Stanley H.E. (1978). Raman spectroscopy: a structural probe of glycosaminoglycans. *Biochimica et Biophysica Acta* 541 (4): 535-542.
- Barret T., Peticolas W. (1979). Laser Raman inelastic light scattering investigations of hyaluronic acid primary and secondary structure. *Journal of Raman Spectroscopy* 8 (1): 35-38.
- Bergholt M.S., St-Pierre J.P., Offeddu G.S., Parmar P.A., Albro M.B., Puetzer J.L., Oyen M.L., Stevens M.M. (2016). Raman spectroscopy reveals new insights into the zonal organization of native and tissue-engineered articular cartilage. *ACS Central Science* 2 (12): 885-895.
- Blundell C.D., Deangelis P.L., Almond A. (2006). Hyaluronan: the absence of amide-carboxylate hydrogen bonds and the chain conformation in aqueous solution are incompatible with stable secondary and tertiary structure models. *Biochemical Journal* 396 (3): 487-98.
- Campos-Casal F.H., Cortez F.A., Gomez E.I., Chamut S.N. (2020). Chemical composition and microstructure of recently oviposited eggshells of *Salvator merrianae* (Squamata: Teiidae). *Herpetological Conservation and Biology* 15 (1): 25-40.
- Carlson G.A., Dragoo J.L., Samimi B., Bruckner D.A., Bernard G.W., Hedrick M., Benhaim P. (2004). Bacteriostatic properties of biomatrices against common orthopaedic pathogens. *Biochemical and Biophysical Research Communications* 321 (2): 472-478.
- Chakrabarti B., Park J.W. (1980). Glycosaminoglycans: structure and interaction. *Critical Reviews in Biochemistry and Molecular Biology* 8 (3): 225-313.
- Chang Y., Chen P.Y. (2016). Hierarchical structure and mechanical properties of snake (*Naja atra*) and turtle (*Ocadia sinensis*) eggshells. *Acta Biomaterialia* 31: 33-49.
- Chen P.Y., McKittrick J., Meyers M.A. (2012). Biological materials: Functional adaptations and bioinspired designs. *Progress in Materials Science* 57 (8): 1492-1704.
- Chen R.F., Wang C.T., Chen Y.H., Chien C.M., Lin S.D., Lai C.S., Wang C.J., Kuo Y.R. (2019). Hyaluronic acid-povidone-iodine compound facilitates diabetic wound healing in a streptozotocin-induced diabetes rodent model. *Plastic and Reconstructive Surgery* 143 (5): 1371-1382.
- Choi S., Han S., Kim N.H., Lee Y.N. (2018). A comparative study of eggshells of Gekkotia with morphological, chemical compositional and crystallographic approaches and its evolutionary implications. *PLOS ONE* 13: 1-31.
- Committee for the Update of the Guide for the Care and Use of Laboratory Animals. (2011). 8th ed., National Academy of Sciences, USA.
- Dicker K.T., Gurski L.A., Pradhan-Bhatt S., Witt R.L., Farach-Carson M.C., Jia X. (2014). Hyaluronan: a simple polysaccharide with diverse biological functions. *Acta Biomaterialia* 10 (4): 1558-1570.
- Di Rienzo J.A., Casanoves F., Balzarini M.G., Gonzalez L., Tablada M., Robledo C.W. InfoStat versin2018. Centro de Transferencia InfoStat, FCA, Universidad Nacional de Córdoba, Argentina. URL <http://www.infoestat.com.ar>
- Donghui F., Beibei W., Zheng X., Qisheng G. (2006). Determination of hyaluronan by spectroscopic methods. *Journal of Wuhan University of Technology-Materials* 21 (3): 32-34.
- Edwards H.G., Hunt D.E., Sibley M.G. (1998). FT-Raman spectroscopic study of keratotic materials: horn, hoof and tortoise shell. *Spectrochimica Acta. Part A, Molecular and Biomolecular Spectroscopy* 54A (5): 745-757.
- Ellis R., Green E., Winlove C.P. (2009). Structural analysis of glycosaminoglycans and proteoglycans by means of Raman microspectrometry. *Connective Tissue Research* 50 (1): 29-36.
- Essendoubi M., Gobinet C., Reynaud R., Angiboust J.F., Manfait M., Piot O. (2016). Human skin penetration of hyaluronic acid of different molecular weights as probed by Raman spectroscopy. *Skin Research Technology* 22 (1): 55-62.
- Euppayo T., Siengdee P., Buddhachat K., Pradit W., Viriyakhasem N., Chomdej S., Ongchai S., Harada Y., Nganvongpanit K. (2015). Effects of low molecular weight hyaluronan combined with carprofen on cani-

- ne osteoarthritis articular chondrocytes and cartilage explants in vitro. *In vitro cellular & developmental biology - Animal* 51 (8): 857-865.
- Fallacara A., Baldini E., Manfredini S., Vertuani S. (2018). Hyaluronic acid in the third millennium. *Polymers* 10 (7): 701.
- Fratzl P., Weinkamer R. (2007). Nature's hierarchical materials. *Progress in Materials Science* 52: 1263-1334.
- Gandhi N.S., Mancera R.L. (2008). The structure of glycosaminoglycans and their interactions with proteins. *Chemical Biology & Drug Design* 72 (6): 455-482.
- Gründelová L., Gregorova A., Mráček A., Vícha R., Smolka P., Minařík A. (2015). Viscoelastic and mechanical properties of hyaluronan films and hydrogels modified by carbodiimide. *Carbohydrate Polymers* 119: 142-148.
- Hallmann K., Griebeler E.M. (2015). Eggshell types and their evolutionary correlation with life-history strategies in Squamates. *PLOS ONE* 10: 1-20.
- Hascall V.C., Majors A.K., de la Motte C.A., Evanko S.P., Wang A., Drazba J.A., Strong S.A., Wight T.N. (2004). Intracellular hyaluronan: a new frontier for inflammation? *Biochimica and Biophysica Acta* 1673: 3-12.
- Heaney R.K., Robinson D.S. (1976). The isolation and characterisation of hyaluronic acid in egg shell. *Biochimica and Biophysica Acta* 451 (1): 133-142.
- Hirsch K.F. (1983). Contemporary and fossil chelonian eggshells. *Copeia* 1983: 382-397.
- Holmes D.F., Lu Y., Starborg T., Kadler K.E. (2018). Collagen fibril assembly and function. *Current Topics in Developmental Biology* 130: 107-142.
- Ingr M., Kutáľková E., Hrnčířík J. (2017). Hyaluronan random coils in electrolyte solutions-a molecular dynamics study. *Carbohydrate Polymers* 170: 289-295.
- Jariyal H., Gupta C., Srivastava A. (2020). Hyaluronic acid induction on breast cancer stem cells unfolds subtype specific variations in stemness and epithelial-to-mesenchymal transition. *International Journal of Biological Macromolecules* 160: 1078-1089.
- Katsumata T., Noguchi S., Yonezawa N., Tanokura M., Nakano M. (1996). Structural characterization of the N-linked carbohydrate chains of the zona pellucida glycoproteins from bovine ovarian and fertilized eggs. *European Journal of Biochemistry* 240: 448-453.
- Karnovsky M.J. (1965). A formaldehyde-glutaraldehyde fixative of high osmolality for use in electron microscopy. *Journal of Cell Biology* 27: 137A.
- Kitagawa T., Hirota S. (2006). Raman Spectroscopy of Proteins. In: *Handbook of Vibrational Spectroscopy, Online*. John Wiley & Sons Ltd., United Kingdom. Pp. 3426-3446.
- Kotzianova A., Rebíček J., Zidek O., Pokorný M., Hrbáč J., Velebný V. (2015). Raman spectroscopy based method for the evaluation of compositional consistency of nanofibrous layers. *Analytical Methods* 7 (23): 9900-9905.
- Kusuda S., Yasukawa Y., Shibata H., Saito T., Doi O., Ohya Y., Yoshizaki N. (2013). Diversity in the matrix structure of eggshells in the Testudines (Reptilia). *Zoological Science* 30: 366-375.
- Lapčik L. Jr., Lapčik L., De Smedt S., Demeester J., Chabreck P. (1998). Hyaluronan: preparation, structure, properties, and applications *Chemical Reviews* 98 (8): 2663-2684.
- Liu Z., Zhang F., Li L., Li G., He W., Linhardt R.J. (2014). Compositional analysis and structural elucidation of glycosaminoglycans in chicken eggs. *Glycoconjugate Journal* 31 (8): 593-602.
- Manes M.E. (2016). Principles for the Productive Breeding of Tegu Lizards. Bilingual Spanish-English Edition, Facultad de Agronomía y Zootecnia, Universidad Nacional de Tucumán, Tucumán, Argentina.
- Manou D., Caon I., Bouris P., Triantaphyllidou I.E., Giaroni C., Passi A., Karamanos N.K., Vigetti D., Theocharis A.D. (2019). The complex interplay between extracellular matrix and cells in tissues. *Methods in Molecular Biology* 1952: 1-20.
- Medina J.M., Thomas A., Denegar C.R. (2006). Knee osteoarthritis: should your patient opt for hyaluronic acid injection? *Journal of Family Practice* 8: 667-675.
- Meziane-Tani M., Lagant P., Semmoud A., Vergoten G. (2006). The SPASIBA force field for chondroitin sulfate: vibrational analysis of D-glucuronic and N-acetyl-D-galactosamine 4-sulfate sodium salts. *The Journal of Physical Chemistry, A* 110 (39): 11359-11370.
- Nusgens B.V. (2010). Acide hyaluronique et matrice extracellulaire: une molécule primitive? [Hyaluronic acid and extracellular matrix: a primitive molecule?]. *Annales de Dermatologie et de Venereologie* 137 (1): S3-S8.
- Nys Y., Gautron J., McKee M.D., Garcia-Ruiz J.M., Hincke T. (2001). Biochemical and functional characterisation of eggshell matrix proteins in hens. *Worlds Poultry Science Journal* 57: 401-13.
- Oleinikov V., Kryukov E., Kovner M., Ermishov M., Tuzikov A., Shiyani S., Bovin N., Nabiev I. (1999). Sialylation sensitive bands in the Raman spectra of oligosaccharides and glycoproteins. *Journal of Molecular Structure* 480-481 (1-3): 475-480.
- Osborne L., Thompson M.B. (2005). Chemical composition and structure of the eggshell of three viviparous lizards. *Copeia* 2005: 683-692.
- Packard M.J., DeMarco V. (1991). Eggshell structure and formation in eggs of oviparous reptiles. In: *Egg incubation: its effects on embryonic development in birds and reptiles*. Deeming D.C., Ferguson M.W.J. (Eds.). Cambridge University Press, Cambridge, United Kingdom. Pp. 53-69.
- Packard M.J., Packard G.C., Boardman T.J. (1982b).

- Structure of eggshells and water relations of reptilian eggs. *Herpetologica* 38: 136-155.
- Parker F.S. (1983). Carbohydrates. In: *Applications of Infrared, Raman, and Resonance Raman Spectroscopy in Biochemistry* 3th ed. Parker F.S. (Ed.), Springer, USA. Pp. 315-347.
- Pike D.A., Andrews R.M., Du W.G. (2012). Eggshell morphology and gekkotan life-history evolution. *Evolutionary Ecology* 26: 847-861.
- Pirnazar P., Wolinsky L., Nachnani S., Haake S., Pilloni A., Bernard G.W. (1999). Bacteriostatic effects of hyaluronic acid. *Journal of Periodontology* 70 (4): 370-374.
- Raman R., Sasisekharan V., Sasisekharan R. (2005). Structural insights into biological roles of protein-glycosaminoglycan interactions. *Chemistry & Biology* 12 (3): 267-277.
- Reineck I., DeAnna J., Suleski T.J., Lee S.A., Rupprecht A. (2003). A Raman study of the hydration of wet-spun films of Li-hyaluronate. *Journal of Biomolecular Structure & Dynamics* 21 (1): 153-157.
- Reisz R.R. (1997). The origin and early evolutionary history of amniotes. *Trends in Ecology & Evolution* 12 (6): 218-222.
- Rizo G., Roldán-Olarte M., Miceli D.C., Jiménez L.E., Álvarez R.M.S. (2016) Structural modifications induced by an in vitro maturation process in zona pellucida glycoproteins of bovine oocytes. A Raman microspectroscopy analysis. *RSC Advances* 6 (86): 83429-83437.
- Rogers M.A., Langbein L., Praetzel-Wunder S., Winter H., Schweizer J. (2006). Human hair keratin associated proteins (KAPs). *International Review of Cytology* 251: 209-263.
- Romanò C.L., De Vecchi E., Bortolin M., Morelli I., Drago L. (2017). Hyaluronic acid and its composites as a local antimicrobial/antiadhesive barrier. *Journal of Bone and Joint Infection* 2 (1): 63-72.
- Rygula A., Majzner K., Marzec K.M., Kaczor A., Pilarczyk M., Baranska M. (2013). Raman spectroscopy of proteins: A review. *Journal of Raman Spectroscopy* 44 (8): 1061-1076.
- Sah M.K., Rath S.N. (2016). Soluble eggshell membrane: A natural protein to improve the properties of biomaterials used for tissue engineering applications. *Materials Science & Engineering. C, Materials for Biological Applications* 67: 807-821.
- Salwowska N.M., Bebenek K.A., Żądło D.A., Wcisło-Dziadecka D.L. (2016). Physiochemical properties and application of hyaluronic acid: a systematic review. *Journal of Cosmetic Dermatology* 15 (4): 520-526.
- Schleich H.H., Kästle W. (1988). *Reptile Eggshells SEM Atlas*. Gustav Fischer, Germany.
- Schmidt-Nielsen K. (1997). *Animal Physiology: Adaptation and Environment*, 5th ed, Cambridge University Press, Reino Unido.
- Scott J.E., Cummings C., Brass A., Chen Y. (1991). Secondary and tertiary structures of hyaluronan in aqueous solution, investigated by rotary shadowing-electron microscopy and computer simulation. *Hyaluronan is a very efficient network-forming polymer. Biochemical Journal* 274 (3): 699-705.
- Scott R.A., Panitch A. (2013). Glycosaminoglycans in biomedicine. *Wiley Interdisciplinary Reviews. Nanomedicine and Nanobiotechnology* 5 (4): 388-398.
- Sekkal M., Dincq V., Legrand P., Huvenne J.P. (1995). Investigation of the glycosidic linkages in several oligosaccharides using FT-IR and FT Raman spectroscopies. *Journal of Molecular Structure* 349 (95): 349-352.
- Sexton O.J., Bramble J.E., Heisler I.L., Phillips C.A., Cox D.L. (2005). Eggshell composition of squamate reptiles: relationship between eggshell permeability and amino acid distribution. *Journal of Chemical Ecology* 31: 2391-2401.
- Sorushanova A., Delgado L.M., Wu Z., Shologu N., Kshirsagar A., Raghunath R., Mullen A.M., Bayon Y., Pandit A., Raghunath M., Zeugolis D.I. (2019). The Collagen Suprafamily: From Biosynthesis to Advanced Biomaterial Development. *Advanced Materials* 31 (1): e1801651.
- Sudha P.N., Rose M.H. (2014). Beneficial Effects of Hyaluronic Acid. In: *Advances in Food and Nutrition Research*, Vol 72, 1st ed. Academic Press. Oxford, United Kingdom. Pp. 137-176.
- Suvarna K., Layton C., Bancroft J.D. (2008). *Bancroft's Theory and Practice of Histological Techniques*, 7th ed., Churchill Livingstone Elsevier, Reino Unido.
- Synytysya A., Synytysya A., Alexa P., Wagner R., Davidková M., Volka K. (2011). Raman spectroscopic study on sodium hyaluronate: an effect of proton and γ irradiation. *Journal of Raman Spectroscopy* 42: 544-550.
- Vuong T.T., Rønning S.B., Suso H.P., Schmidt R., Prydz K., Lundström M., Moen A., Pedersen M.E. (2017). The extracellular matrix of eggshell displays anti-inflammatory activities through NF- κ B in LPS-triggered human immune cells. *Journal of Inflammation research* 10: 83-96.
- Wang W., Zhang M., Lu W., Zhang X., Ma D., Rong X., Yu C., Jin Y. (2010). Cross-linked collagen-chondroitin sulfate-hyaluronic acid imitating extracellular matrix as scaffold for dermal tissue engineering. *Tissue engineering. Part C, Methods* 16 (2): 269-279.
- Weinkamer R., Fratzl P. (2011). Mechanical adaptation of biological materials. The examples of bone and wood. *Materials Science and Engineering: C* 31 (6): 1164-1173.
- Widjaja E., Garland M. (2010). Detection of bio-constituents in complex biological tissue using Raman microscopy. Application to human nail clippings. *Talanta* 80 (5): 1665-1671.
- Yuen S.N., Choi S.M., Phillips D.L., Ma C.Y. (2009).

- Raman and FTIR spectroscopic study of carboxymethylated non-starch polysaccharides. *Food Chemistry* 114: 1091-1098.
- Zhao Y.H., Chi Y.J. (2009). Characterization of collagen from eggshell membrane. *Biotechnology* 8: 254-258.
- Zhu G., Zhu X., Fan Q., Wan X. (2011). Raman spectra of amino acids and their aqueous solutions. *Spectrochimica Acta. Part A, Molecular and Biomolecular spectroscopy* 78 (3): 1187-1195.
- Zhu Z., Wang Y.M., Yang J., Luo X.S. (2017). Hyaluronic acid: a versatile biomaterial in tissue engineering. *Plastic and Aesthetic Research* 4: 219-227.